Trends in fire characteristics in the partially vegetated dunes of the southwest Kalahari Desert

Rosemary A. Huck*[a,b,i], Giles F.S. Wiggs[a], David S.G. Thomas[a]

[a] School of Geography and the Environment, University of Oxford, South Parks Rd, Oxford OX1 3QY
[b] School of Geography and Environmental Science, University of Southampton
[i]School of Geography and the Environment, University of Oxford, South Parks Rd, Oxford OX1 3QY
**Corresponding author*. Email address: rosemary.huck@ouce.ox.ac.uk

Abstract

Fire is often cited as a major disturbance that can induce increased aeolian activity on vegetated sand dunes due to the removal of protective plant cover. This study

investigated the spatial and temporal dimensions of burning as an agent of disturbance in partially vegetated linear dunes in the southwest Kalahari. The region is often omitted as a burn-prone area in continental and global burned area studies due to its aridity and proximity to intense temperate zone fires. The MODIS burned area product was used to create an inventory of burned area from 2000-2023 to identify trends in burned area extent and occurrence. In addition, MODIS-derived Soil Adjusted Total Vegetation Index (SATVI) was used to calculate vegetation recovery post-burn. 13,310 km^2 of the southwest Kalahari dune field burned over the 24-year study period; 11.1% of the total area. The land management regime significantly impacted on fire frequency ($p < 0.001$) and size ($p < 0.001$), with more burns occurring on privately owned land but larger burns within the Kgalagadi National Park. It also significantly affected burn duration ($p < 0.001$), with the National Park having longer lasting burns. Vegetation recovery is swift after burning, with cover returning to control levels within about two years of being burned. This study highlights how the temporal and spatial disturbance effect of the fire is limited by land management in the study region and rapid vegetation recovery post-burn.

Key words:
Landscape fire; *disturbance*; *sand dunes*; *land use*; *Kalahari*

Highlights:

1. Fires are a significant disturbance in the southwest Kalahari linear dune system
2. Fire occurrence, size, and duration are impacted by land management
3. Vegetation recovery is swift, with return to control levels in under two years

1 Introduction

In desert dune environments, aeolian processes dominate sediment distribution and are a fundamental factor in biogeochemical cycles and geomorphological patterns (Okin et al., 2006). Vegetation on dunes can affect the ability of the wind to move sediment by reducing the erodibility of the surface through physical sheltering or

binding of sediments, and by reducing the erosivity of the wind by increasing the aerodynamic roughness (Leenders et al., 2007; Wiggs et al., 1995). Additionally, biological soil crusts (biocrusts) play an important role in stabilising dune surfaces and reducing sand movement (Levin et al., 2012; Thomas and Dougill, 2007). Landscape-scale dune surface activity has been framed according to vegetation cover (Livingstone and Thomas, 1993): 'active' dunes are often bare or with low vegetation density, and have high levels of aeolian erosion; 'fixed' or 'inactive' dunes have higher vegetation densities and are considered stabilised with limited aeolian erosion. Consequently, both states will stay in equilibrium unless disturbed (Bhattachan et al., 2014).

Disturbance events are classed as events which cause a perturbation to a component of the system (Rykiel, 1985) and in vegetated dunes include the loss of stabilising vegetation through drought, grazing, or fire amongst other factors. Wiggs et al., (1995) found a non-linear relationship between mean vegetation cover and surface activity in the southwest Kalahari and noted that when cover falls below 14% on the crest and upper flanks of the dune then surface activity increases markedly. Although there is no simple threshold of vegetation cover below which surface activity begins as transport can happen at high surface coverage (especially under high wind stress), the effective threshold of 14% surface cover is a useful indicator for surface activity at the dune scale (Wiggs et al., 1995). Once vegetation is disturbed beyond a critical threshold, positive feedback mechanisms can push a system that was previously stable to an alternative stable state (i.e., from inactive to active; Bhattachan et al., 2014). Vegetated or partially-vegetated dune systems are a

significant feature of many dryland landscapes, and fire is considered to be a significant mechanism for vegetation destruction and increase in wind-erosion in dryland environments (Miller et al., 2012; Wasson and Nanninga, 1986).

Once a sand surface has become activated, saltation bombardment by sand can cause mechanical injury to vegetation, increasing vegetation mortality and limiting the regrowth of plants (Strong et al., 2010). Dunes can become taller and steeper (Hesse and Simpson, 2006), and surfaces may become active dust sources (Sweeney et al., 2023), which can have detrimental effects on local air quality and human health (Goudie, 2014). The incineration of vegetation releases previously trapped sediment and modulates airflow which can lead to an increase in the erosive power of the wind (Okin et al., 2009). In addition, fire changes the erodibility of the surface through inducing soil hydrophobicity (Ravi et al., 2009). The duration of increased aeolian activity is linked to the length of time in which vegetation can recolonise the burned area. In the linear dune systems of the Kalahari and Simpson Deserts the recovery time has been posited to be around five and over six years respectively (Strong et al., 2010; Wiggs et al., 1994) but some estimates place recovery times to be as high as 25-30 years (Levin et al., 2012). Therefore, defining the magnitude, both spatially and temporally, of state-changing vegetation disturbances can allow a better quantification of the significance of the disturbance on a landscape.

Climate oscillations and weather are important controls on fire activity (Pricope and Binford, 2012). For significant burning to occur fires require biomass accumulation, atmospheric conditions conducive to burning (e.g., dry and windy), and an ignition

120 event (Moritz et al., 2012). Over short timescales, precipitation can limit fire ignition
121 and extent, and over longer periods climatic oscillations can lead to biomass
122 accumulation in the wet season and increased fuel accumulation for burning during
123 drier periods (Pricope and Binford, 2012).
124
125 In the vegetated linear dune system, extended dry seasons, predominantly grass
126 ecosystems, combined with the arid environment and extended dry seasons, leads to
127 surfaces being vulnerable to burning. Furthermore, fire occurrence, extent and
128 severity are affected by a mixture of both natural, and anthropogenic factors. For
129 example, fires are ignited through both natural (e.g., lightning) and anthropogenic
130 (e.g., cigarette stubs, vehicle sparks) causes and, under dry and windy conditions,
131 can spread quickly.
132
133 For decades, mapping burned area and quantifying the impact of burning on the
134 environment at a range of scales has been a focus for interdisciplinary studies
135 (Barbosa et al., 1999; Giglio et al., 2018). These studies are often conducted at global
136 to continental scale, and burned area representation in figures often highlights the
137 intensity of fire in more woodier or temperate regions (e.g., Andela and Van Der
138 Werf, 2014; Khairoun et al., 2024) or over short timescales (e.g., Chuvieco et al.,
139 2022). As a result of these scaling decisions there is frequent omission of some arid
140 areas as burn-prone regions (Andela and Van Der Werf, 2014; Jones et al., 2022).
141
142 A growing body of research addresses post-fire aeolian erosion in arid environments
143 (e.g., Huck et al., 2025; Sankey et al., 2012). Research has also addressed some drivers

of disturbance on vegetated linear dunes including increased aridity (Thomas et al., 2005) and grazing pressure (Bhattachan et al., 2014). Fire is often cited as being a major disturbance that can induce increased aeolian activity on sand dunes (e.g., Hugenholtz and Wolfe, 2005). There has, to date, been little assessment of the scale of fire as a disturbance factor on vegetated sand dunes. Here, we aim to investigate the scale of burning as an agent of disturbance in partially vegetated dunes in the southwest Kalahari. This aim is achieved through creating an inventory of fire from 2000-2023 to identify trends in burned area extent and occurrence.

2 Study area

The southwest Kalahari dune field (Figure 1) covers ~120,200 km^2 with linear dunes dominant in cover the western portion of the Kalahari Sand Sea in eastern Namibia, the Northern Cape of South Africa and southwest Botswana before degrading to dune-like patterns resembling barchanoid ridges to the east (Bullard et al., 1995). The most common dune form in the study area is classified as vegetated linear dunes which extend mainly in a NNW to SSE orientation (Bullard et al., 1995).

Today much of the southwest Kalahari linear dune field comprises agricultural land, which is either privately owned or community-administered and used for livestock production, herein 'primarily private farmland' (PPF). The exception is the Kgalagadi Transfrontier Park (KTP), located in the Northern Cape of South Africa and across the border into Botswana (Figure 1). The two different land uses have differing fire management policies. Since colonial times the Namibian national fire policy has been to avoid fires, a policy still enforced amongst local landholders as

fire can have devastating effects for agriculture, property, and grazing (Humphrey et al., 2021). The Kgalagadi Transfrontier Park fire policy dictates that fires that burn in the dry season are allowed to burn until they self-extinguish (Spies et al., 2016).

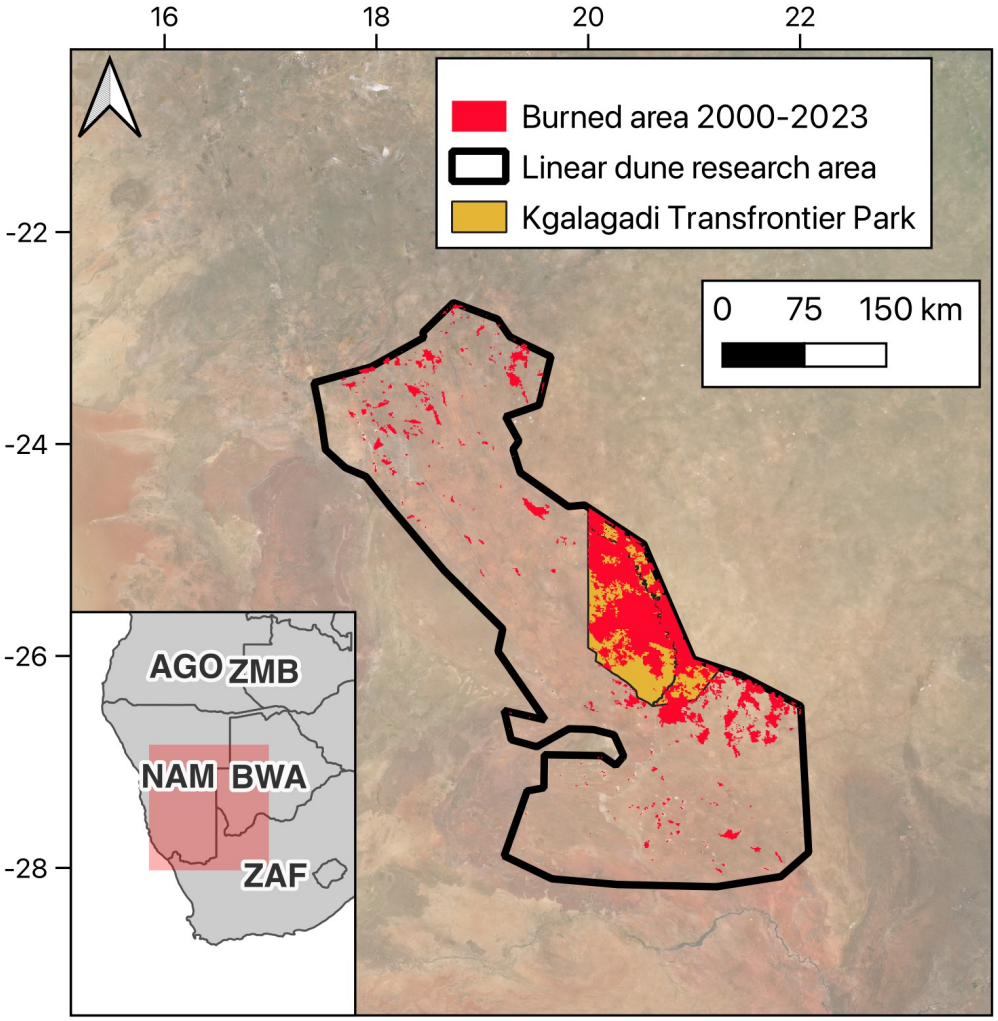

Figure 1. Fire in the southwest Kalahari dune field. The study area of interest outlined in black and all burned land delineated by the MODIS BA product from 2000 to 2023 are displayed in red. The Kgalagadi Transfrontier National Park is highlighted in orange. Image © 2023 Planet Labs PBC (Planet, 2017).

The typical vegetation in the study area is Kalahari Xeric Savanna (van Rooyen and van Rooyen, 1998), a mix of annual grasses (mainly *Schmidtia kalahariensis*), perennial grasses (e.g., *Eragrostis lehmanniana*), shrubs (e.g., *Acacia mellifera)* and sparsely

populated trees (e.g., *Acacia erioloba*). The dominance of annual grasses, particularly in the farmland, leads to an annual build-up of dead and dry vegetation that are easily combustible. The vegetation is very sensitive to changes in climatic and physical conditions and therefore coverage is dynamic in both time and space through complex relationships between sediment, plants, temperature, grazing pressure, and wind erosion processes (Smit et al., 2024). The ephemeral nature of vegetation cover provides a unique biogeomorphological landscape on which fires can develop. The ability of a fire to spread laterally is restricted by the vegetation state of the dune crests, as fire often cannot spread across large unvegetated crests (Burrows et al., 2009).

The study area today exhibits a strong north-south precipitation gradient (Figure 2), with the northern region receiving more precipitation linked to the seasonal movement of the Inter-Tropical Convergence Zone (Kaseke et al., 2016). The region has large interannual variability in precipitation but generally the year can be classified into three seasons: cold and dry in May to August, hot and dry in September to December, and hot and wet in January to April (van Rooyen and van Rooyen, 1998). Herein we refer to the cold and dry and the hot and dry seasons as the 'dry season' and the hot and wet season as the 'wet season'. In wet years biomass can build up, whereas in dry years without disturbance biomass will remain constant or reduce. The El Niño-Southern Oscillation (ENSO) modulates precipitation patterns over differing oscillations to induce drought or intensify wet season rainfall which can further build biomass and affect interannual variability in fuel load and subsequent burning (Andela and Van Der Werf, 2014; Swetnam and

Betancourt, 1990). In southern Africa, ENSO influence on surface temperature is strong and is triggered by the sea surface temperatures in the Indian Ocean the preceding December (Manatsa and Reason, 2017). Therefore, water resources in the region fluctuate with ENSO oscillations with extreme cycles resulting in El Niño and La Niña phases (Manatsa and Reason, 2017). El Niño phases have been linked to a decrease in precipitation, drought, and a reduction in vegetation (Hao et al., 2020) and La Niña phases have been linked to increased precipitation (Mphale et al., 2014) in the region.

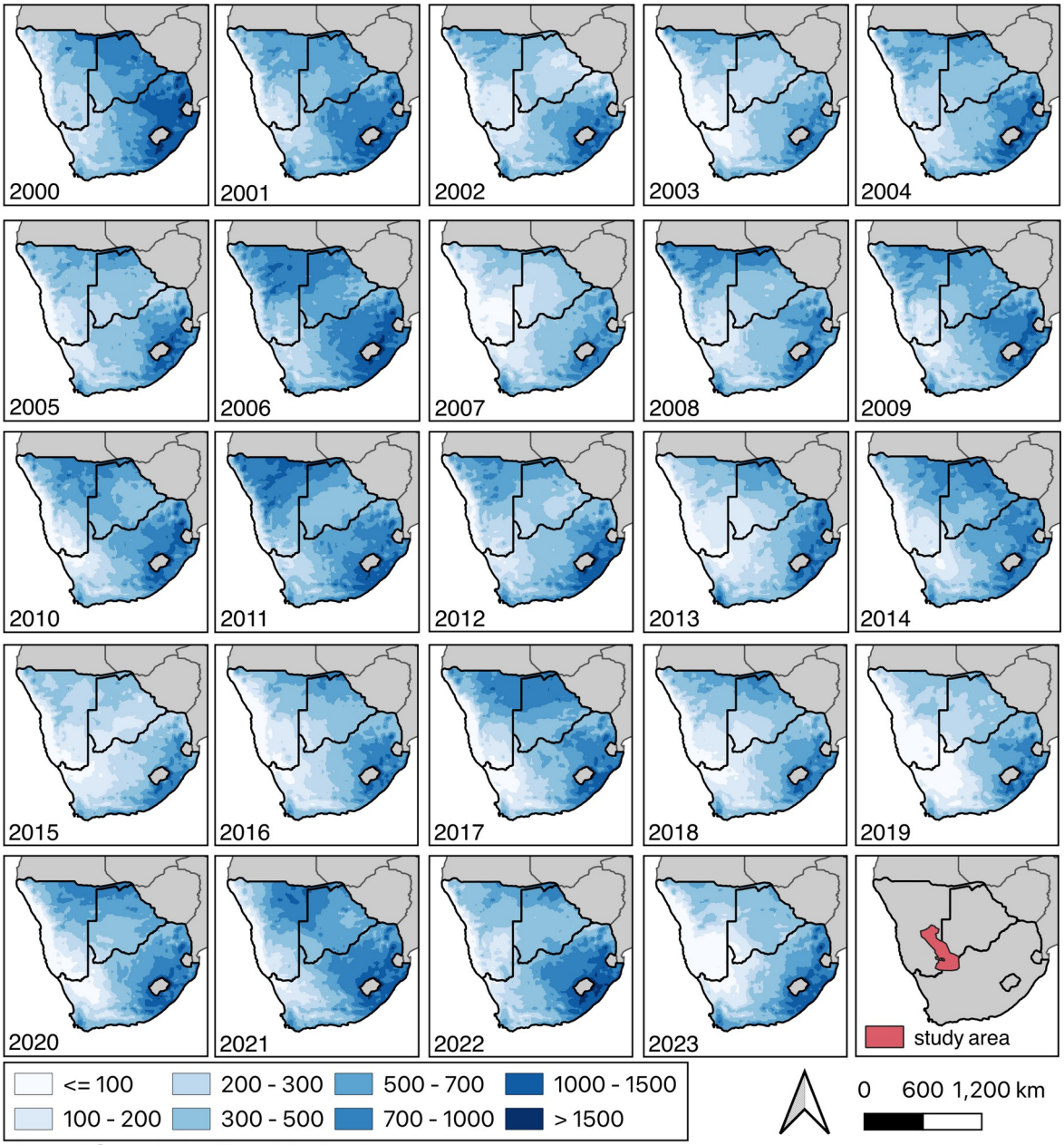

Figure 2. Annual cumulative precipitation (mm) in Namibia, Botswana, and South Africa using ERA5-Land reanalysis data from 2000 - 2023 (Muñoz-Sabater et al., 2021). Dry years, (2003, 2007, 2013 – 2016, 2018 - 2020, and 2023) although less common, often indicate drought conditions such as the 2018 to 2020 southern Africa drought. Whereas wet years (2000 – 2002, 2004 - 2006, 2008 - 2012, 2017, and 2021 - 2022) are more frequent but range in cumulative precipitation. For example, there was an extremely yet season in 2006 and a more moderate wet season in 2008.

3 Methods

3.1 Burned Area

The MODIS Burned Area (BA) Product (MCD64A1 Version 6.1; Giglio et al., 2018) is a popular tool for the detection of burned land area (e.g., Jones et al., 2022; Roy et al., 2008). The product estimates the daily burned area through rapid changes in daily surface reflectance at 500 m resolution globally from the year 2000 to the present (Giglio et al., 2018). The MODIS BA tool has been useful for global fire trend studies (e.g., Jones et al., 2022; Van Der Werf et al., 2010) to build a picture of fire occurrence, controls, and trends. But, like many satellite-derived measurements, the MODIS BA product still has a variety of limitations (Chuvieco et al., 2019). These can lead to commission errors (false-positives) and omission errors (false-negatives) and may form due to satellite over-pass frequency and diurnal timing, cloud cover, and the low spatial resolution of the algorithm (Jones et al., 2022). These errors do not occur uniformly across the globe, due to cloud cover and over-pass frequency, and detection rates in southern Africa sit at approximately 85% of the true burned area (Archibald et al., 2009). Another known limitation of coarse-resolution BA products, such as MODIS BA, struggle to detect small fires < 500 m^2, which leads to an underestimation of the true burned area (Khairoun et al., 2024). Despite these limitations, the MODIS BA product provides a succinct fire detection tool for the last 24 years, particularly in hard-to-access areas, which can give useful insights into fire that could not be achieved with local inventories of fire activity (Jones et al., 2022). Here, we use the MODIS BA product to achieve an overall image of fire activity on the Kalahari linear dunes for the last 24 years to assess trends in occurrence and extent.

To mitigate the effect of any commission errors within the fire count, each burn recording from the MODIS BA data was individually assessed for the possibility of the MODIS BA algorithm returning a false-positive. For example, a high number of pixels identified as burned were found in pans (deflation basins that can have seasonal inundation of surface water, but which are usually dry; Goudie,1991) in the South African area of the study. Burn pixels that were found within pans were removed due to the low likelihood that they represented fires, as many pan surfaces have less than 10%, and often zero vegetation cover (Leistner, 1959) but can experience rapid changes in surface reflectance when they flood, potentially triggering the MODIS algorithm to detect fire on the pans.

Once the commission errors were removed, these data were then assessed for fires that were burning on multiple fronts or over many days which returned numerous unconnected pixels and increasing the total burn count. The fires that were burning on multiple fronts were classed as one burn in the count, determined by looking at the previous day's burned pixels and assessing if the current day pixels were connected. However, each individual day the continuing fire burned was counted as a new burn in the count. Following this method causes large size burns to only count as a singular burn, leading to difficulty differentiating between large and small burns which can have vastly different effects in terms of scale of disturbance. Therefore, to quantify the spatial and temporal scale of fire as a disturbance effect on the landscape, a combination of both daily burn count, daily burned area, and burn duration was used in this study. Fire counts where multi-day fires are displayed as a single burn event are presented in Figure S2.

Data were then gridded to 0.5˚ by 0.5˚. The count for each grid cell with overlapping burned area was then calculated to compile how many separate days over the study period the cell burned. The shortest gap between burn years for each fire within a cell was used to estimate reburn time. Each grid cell covers ~113 km^2, and there is the possibility that the two separate fires that are counted as reburning do not have any overlap. Further, by scaling reburn at a yearly scale, fires that burned in the same fire season (for example December 2021 and January 2022) would count as a reburn. If fires are large and burn slowly for an extended period, then they may be detected as reburned areas. The majority of the pixels that have a less than 5-year reburn time, burned in two separate fires in September 2022 and September 2021. These two fires burned within the same pixel, but not necessarily the same area on the ground.

3.2 Climate data

Globally there is a link between vegetation fire occurrence and ENSO extreme phases (Andela and Van Der Werf, 2014). To assess any relationship between fires and ENSO extreme phases in the study area, monthly ENSO occurrence data was downloaded from the National Oceans and Atmosphere Administration's (NOAA) Climate Prediction Center (CPC; dataset available at https://origin.cpc.ncep.noaa.gov/products/analysis_monitoring/ensostuff/ONI_v5.php). Each month was classified into El Niño, La Niña, or no occurrence. Further, to assess if there is any delayed impact of ENSO on fire in the region, 1-month, 6-month, 12-month, and 18-month lags were introduced and tested. Due to

the non-normality of the data, Kruskal-Wallis rank sum tests were performed to assess the statistical relationships between the ENSO and the burn count, burned area, and burn duration for the whole study area, the Kgalagadi Transfrontier Park, and the primarily private farmland.

3.3 Vegetation indices

To investigate how long the surface is devoid of protective vegetation (both alive and dead) after fire, 17 fire scars were selected to track throughout the study period. Each burn required an area larger than one kilometre to be tracked and there needed to be no evidence of previous burning (verified through the MODIS BA product for fires after 2009 or Google Earth before 2009). The coordinates of each fire scar are listed in Table 1 and displayed in Figure S1. Each of these scars were then co-located with an adjacent unburned (termed control) area for comparative purposes. These corresponding 17 control locations are situated more than 500 m outside of the fire scar to ensure they were in a different pixel of MODIS imagery.

MODIS Surface reflectance product (MOD09GA) provides daily, 500 m resolution surface reflectance for MODIS bands 1- 7. To obtain consistent above-ground biomass estimates for the sites, we calculated the Soil Adjusted Total Vegetation Index (SATVI; Marsett et al., 2006) for each daily MOD09GA image. SATVI is calculated as:

$$SATVI = \frac{SWIR1 - R}{SWIR1 + R + L}(I + L) - \frac{SWIR2}{2}$$

Equation 1.

Where SWIR1 = MODIS shortwave infrared Band 6, R = MODIS Red Band 1, and SWIR2 = MODIS shortwave infrared Band 7. L is a soil-adjustment factor between 0 and 1. The L value of 0.5 was used in this study, representing a moderate vegetation coverage. The SATVI index returns a value between -1 (no vegetation) and 1 (green vegetation). As this study is primarily interested in the post-fire period where the surface available to be eroded by the wind, the use of SATVI is satisfactory here.

SATVI has been shown to be more sensitive to changes in vegetation than other commonly-used vegetation indices, such as the Normalised Differenced Vegetation Index (NDVI) or the Enhanced Vegetation Index (EVI; Goirán et al., 2012). This enhanced detection can be attributed to SATVI utilising shortwave Infrared (SWIR) bands which are sensitive to both green and senescent vegetation, as opposed to NDVI and EVI which rely on near infrared for green vegetation only. The sensitivity to non-green vegetation cover has made SATVI a useful tool in arid environments where vegetation is senescent for much of the year (Marsett et al., 2006; Poitras et al., 2018). NDVI and EVI calculated with MODIS MOD09GA 16-day tool for each tracked fire scar were originally calculated for this study as well but ultimately were excluded due to the lack of sensitivity to changes in vegetation in arid environments. However, the workflow for the data was established whilst still including NDVI and EVI data. To match MODIS product EVI and NDVI sample temporal resolution, the SATVI data were reduced to 16-day mean reflectance. As a result, all SATVI vegetation values are presented with the systematic error window of ±16 days.

The percent cover of both green and senescent vegetation can be estimated using the maximum and minimum SATVI values to calculate the Total Vegetation Fractional Cover (TVFC; Villarreal et al., 2016). Here, the maximum and minimum value of each individual pixel was used to calculate the TVFC which across all the cells ranged from a minimum of -0.2852 to a maximum of -0.0729. TVFC is calculated as:

$$TVFC = \frac{SATVI - SATVI_{min}}{SATVI_{max} - SATVI_{min}} X\ 100$$

Equation 2.

By utilising TVFC, a value of 100% TVFC represents the maximum vegetation cover within the pixel during the measurement period and should not be interpreted as 100 % surface cover. SATVI derived TVFC is a useful metric for establishing the extent to which burning alters vegetation cover but does not provide information on the change in vegetation structure. Correlations between SATVI derived TVFC and field measurements by Villarreal et al. (2016) were weak, indicating that the relationship between the index and the actual surface cover is not well constrained. Subsequently the results should be interpreted as indicative of relative, rather than absolute, changes in cover and subject to uncertainty.

Table 1. The 17 tracked fires and corresponding control coordinate and date of fire.

Fire	Year	Fire Day Of Year	Date of fire	Burned Coordinates	Control Coordinates
1	2001	283	10/10/2001	-23.886108, 18.27055	-23.88191, 18.32897
2	2006	199	18/07/2006	-23.80115, 18.581572	-23.79735, 18.544
3	2006	278	05/10/2006	-23.47634, 18.34874	-23.43737, 18.41622
4	2007	263	20/09/2007	-24.525542, 18.712428	-24.53783, 18.68606
5	2007	295	22/10/2007	-24.983461, 20.024239	-24.98885, 20.080366
6	2007	25	25/01/2007	-27.075864, 20.619525	-27.06651, 20.64863
7	2009	258	15/09/2009	-24.985778, 20.246531	-24.917485, 20.331255

8	2010	280	07/10/2010	-27.690119, 21.335681	-27.65235, 21.37921
9	2011	204	23/07/2011	-23.589586, 18.6381	-23.5826, 18.68335
10	2011	254	11/09/2011	-24.885406, 18.864719	-24.8703, 18.88918
11	2011	270	27/09/2011	-25.306547, 20.199558	-25.25766, 20.21641
12	2012	306	01/11/2012	-23.178489, 18.533536	-23.21355, 18.62934
13	2012	262	18/09/2012	-26.09055, 20.597092	-26.19015, 20.52438
14	2013	56	25/02/2013	-27.818025, 21.595753	-27.86208, 21.60531
15	2017	228	16/08/2017	-23.976797, 18.532275	-23.9993, 18.4908
16	2017	206	25/07/2017	-27.4131, 20.608086	-27.379528, 20.574417
17	2018	299	26/10/2018	-27.065808, 20.642625	-27.072131, 20.666761

4 Results

4.1 Spatial trends of burning

Over the 24-year study period 13,310 km^2 of the southwest Kalahari dune field burned, 11.1% of the total area. When including land that burned more than once over the study period, 16,125 km^2 burned in 240 individual burn events over 417 days. Figure 3 illustrates the highly concentrated spatial organisation of fire on the linear dunes. There are few cells where only single burns occur; if a fire is detected within a grid cell 66% of the time either the burn continues for more than one day or has multiple burn events over the study period. Of the overall burned area, a substantial portion, 10,625 km^2 (65.8%), burned in the Kgalagadi Transfrontier Park. Fires within the Kgalagadi Transfrontier Park burned for a median time of six days compared to two days on the primarily private farmland. These long duration burns are combined with the multiple fires in different years and result in the high number of burn days in the Kgalagadi Transfrontier Park (Figure 3). The highest density of burns occurred along the Nossob River, which is the boundary between South Africa and Botswana and a road in the Kgalagadi Transfrontier Park. There is also another small cluster of burned area in the wetter (see Figure 2) northern part of the research area, where burns were observed multiple times within the 0.5˚ pixels.

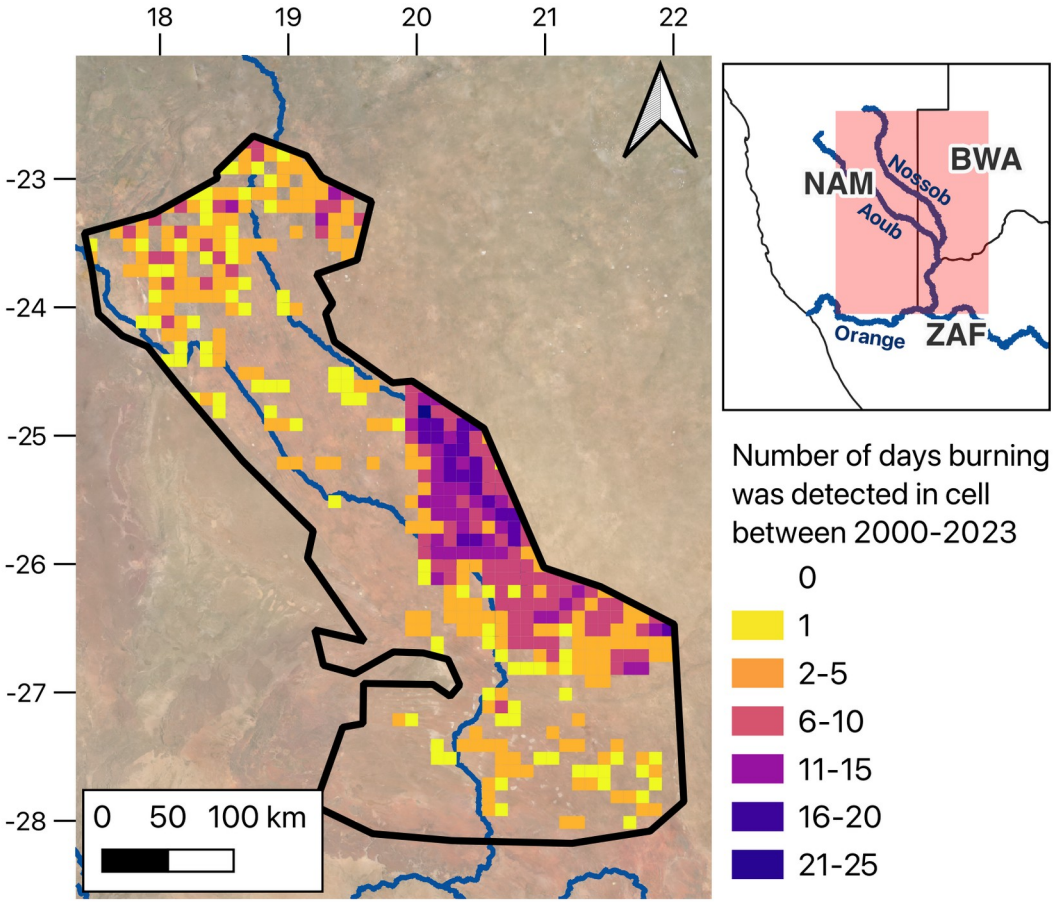

Figure 2. Number of days burning was detected in the 0.5° cell between 2000 - 2023. Background image © 2023 Planet Labs PBC.

4.2 Temporal trends of burning

There is marked interannual variability in burn counts (Figure 4), with the highest total number of burns in both land use classifications recorded in 2022, with 77 burn days compared to no burns at all being recorded in 2004, 2005, and 2016. No obvious regular cycle is evident, with peaks occurring in 2012, 2021, and 2022. The largest number of burns in a month was recorded in September 2021 with 28 burning days. At the monthly scale, the maximum burned area and burn counts tend to cluster

around September in the early dry season (Figure 4). Wet season burns make up only 25% of the burning days.

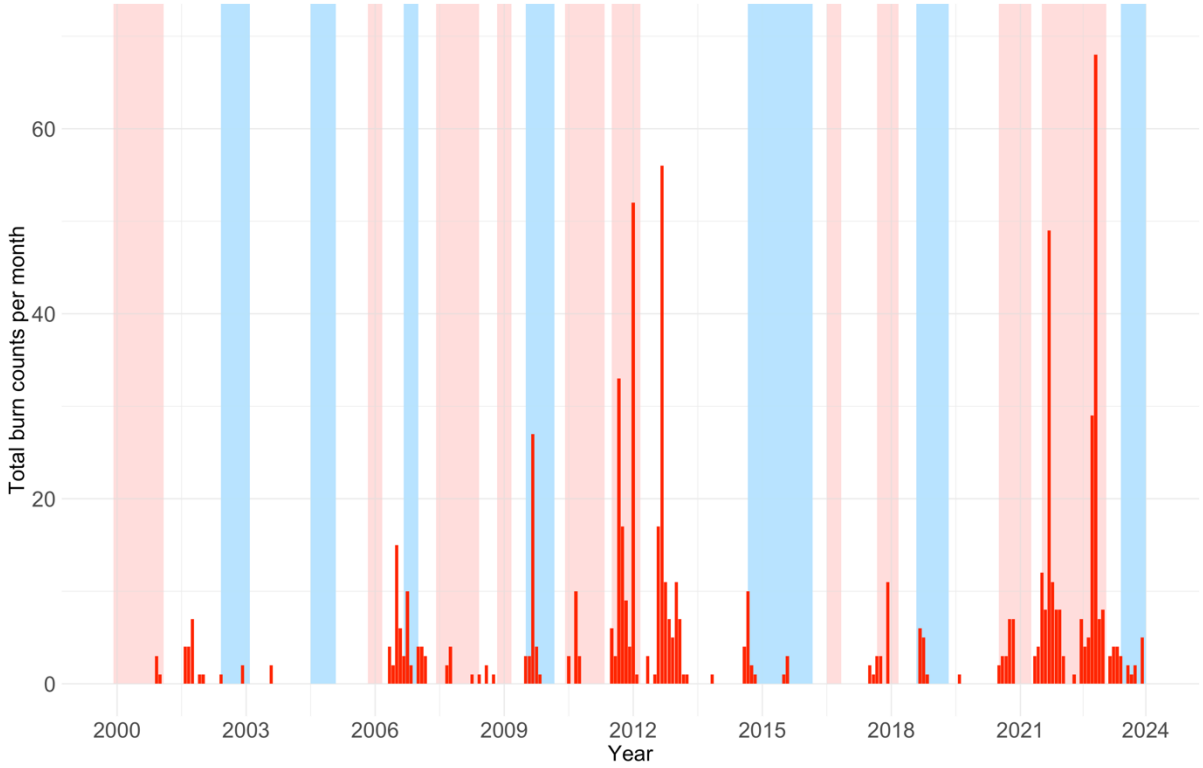

Figure 3. Total burn counts per month over the 24-year study period for the whole study area. Overlayed are the ENSO periods, with El Niño months in blue, and La Niña months in red.

Figure 5 illustrates the importance of representing both burn count and burned area, as different land management regimes display opposing trends. The Kgalagadi Transfrontier Park has a relatively low daily burn count, but a large burned area. Contrastingly, the primarily private farmland has a high burn count, but these burns are small. These are not the only difference in patterns observed between the two land management regimes. The primarily private farmland has more isolated burn incidences throughout the year, with the highest frequency of burning occurring in September which is the middle of the dry season (Figure 5). However, sporadic burns still happen throughout the wet season. Conversely, burns in the Kgalagadi

Transfrontier Park observe a distinct fire season, which peaks in September through to October but tends to be limited in number, burn for a longer time, and over a larger area. There is also a second fire window in late January, where fires have burned on multiple years.

Kruskal-Wallis tests showed that there was significant difference between the Kgalagadi Transfrontier Park and the primarily private farmland in the monthly burn count ($p < 0.001$), monthly burn duration ($p < 0.001$) and monthly burned area ($p < 0.001$).

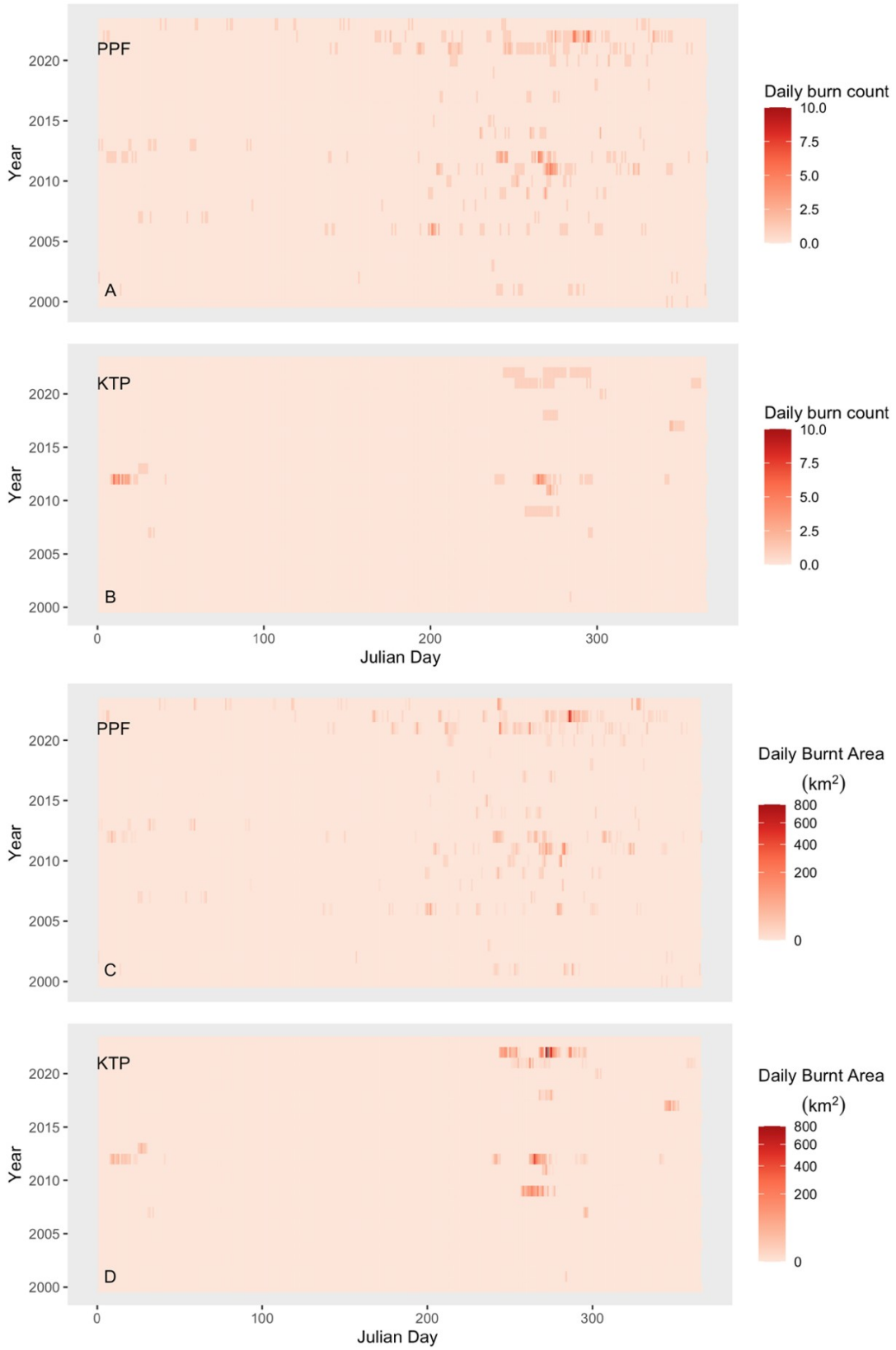

Figure 4. Daily burn count (Panels A&B) and burned area (Panels C&D) from 11/01/2000 to 31/12/2023 using cleaned MODIS burned area product in research area (see Figure 1) for the primarily private farmland (PPF; Panels A&C) and the Kgalagadi Transfrontier Park (KTP; Panels B&D).

4.3 ENSO phases

Fires burned in all ENSO phases (Figure 4). Multiple, successive months of burn counts are observed in neutral ENSO months in 2002 and 2012, in El Niño conditions in 2014 and 2019, and during La Niña phases of 2012, 2021, and 2022. Fire counts peak in October 2022 and January and September 2012 which are all in La Niña months. The largest fires do not burn after long periods without a La Niña extreme phase (Figure 4). Years with the highest fire counts often occur after two consecutive La Niña phases.

Overall, fires occur more frequently and burn a larger area during La Niña conditions (Figure 6). However, burns within land management systems also display different trends within the ENSO oscillations (Figure 6). Sensitivity to ENSO is particularly evident in the Kgalagadi Transfrontier Park burn trends, which can be considered an emulation of a more 'natural' cycle of fire in the area. Within the Kgalagadi Transfrontier Park, there is a delayed onset from the beginning of a La Niña phase and the occurrence of burns. Land outside of the Kgalagadi Transfrontier Park has a higher number of burns occurring in the neutral ENSO months, but this is not reflected in the burned area, suggesting small frequent burns. There is no significant effect of the current ENSO stage on the burned and control pairs ($p > 0.05$; Table 2). However, ENSO stage has a significant effect on the burned area and fire count when lagged by 6 and 12 months ($p < 0.005$; Table 2). There is no evidence in the data analysed that burn duration is not impacted by the current or lagged ENSO cycle.

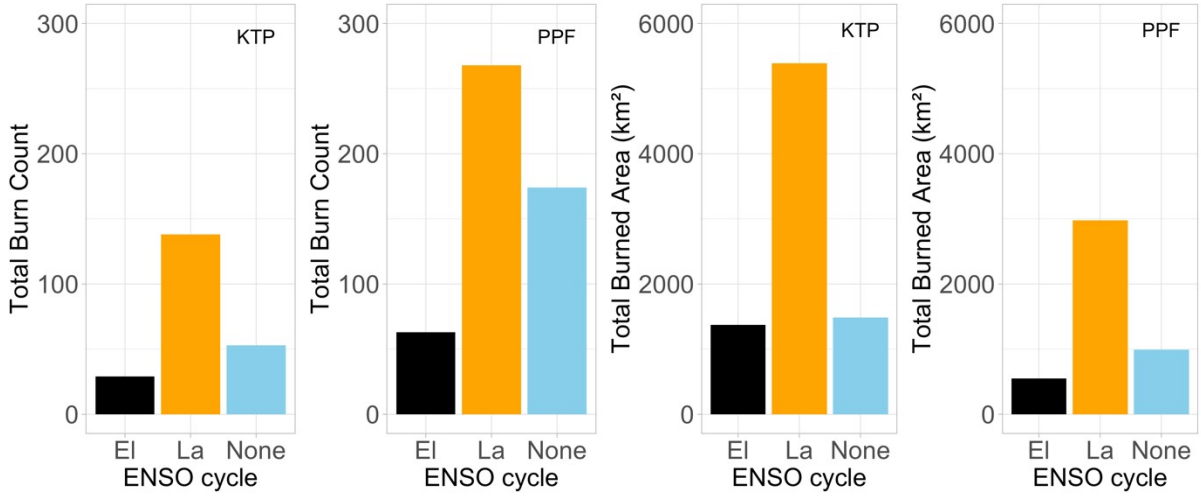

446

447 **Figure 5.** Total burn count and total burned area for the Kgalagadi Transfrontier Park (KTP)
448 and primarily private farmland (PPF) under different ENSO oscillations. El Niño conditions
449 are in Black, La Niña conditions are in orange, and neutral is in blue.

450

451 **Table 2.** Relationship between ENSO current and lagged phases for the whole study area,
452 Kgalagadi Transfrontier Park, and primarily private farmland against the monthly burn
453 count, burned area, and burn duration using Kruskal-Wallis rank sum test.

K-W test	Lag time (months)	Whole study area	Kalagadi Transfrontier Park	Primarily Private Farmland
Burn count	0	$p > 0.05$	$p > 0.05$	$p > 0.05$
Burned area	0	$p > 0.05$	$p > 0.05$	$p > 0.05$
Burn duration	0	$p > 0.05$	$p > 0.05$	$p > 0.05$
Burn count	1	$p > 0.05$	$p > 0.05$	$p > 0.05$
Burned area	1	$p > 0.05$	$p > 0.05$	$p > 0.05$
Burn duration	1	$p > 0.05$	$p > 0.05$	$p > 0.05$

Burn count	6	**p < 0.005**	**p < 0.05**	**p < 0.005**
Burned area	6	**p < 0.005**	**p < 0.05**	**p < 0.005**
Burn duration	6	p > 0.05	p > 0.05	p > 0.05
Burn count	12	**p < 0.005**	**p < 0.005**	**p < 0.005**
Burned area	12	**p < 0.005**	**p < 0.005**	**p < 0.005**
Burn duration	12	p > 0.05	p > 0.05	p > 0.05
Burn count	18	p > 0.05	p > 0.05	p > 0.05
Burned area	18	p > 0.05	p > 0.05	p > 0.05
Burn duration	18	p > 0.05	p > 0.05	p > 0.05

4.4 Reburning

The areas that reburn are clustered within the Kgalagadi Transfrontier Park, where some areas reburned after less than a year. This rapid reburning mainly occurred in the 2020/21 and 2021/22 dry seasons when two large fires swept through the Kgalagadi Transfrontier Park in successive years. 59.6% of the pixels in the Kgalagadi Transfrontier Park burned over multiple incidences, Figure 7 only displays the shortest time to a reburn for a fire within a pixel. Most of the Kgalagadi Transfrontier Park reburned in the study period in less than 10 years. Outside the

Kgalagadi Transfrontier Park, some areas reburned, but there was a large variability in time between burns. There is a concentration of reburned areas in the wetter north of the linear dune system. There are a few isolated incidents of reburning on farmland in the South African portion of the linear dunes.

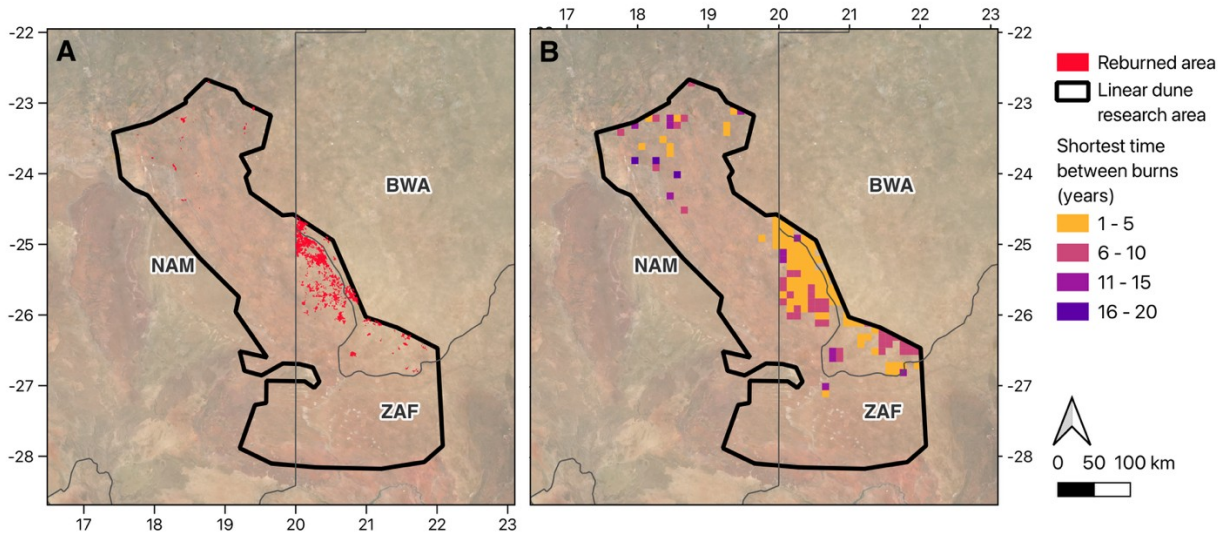

Figure 6. Reburned area (Panel A) and the shortest number of years between burning for all the fires detected in each 0.5˚ cell between 2000- 2023 (Panel B). Background image © 2023 Planet Labs PBC.

4.5 Vegetation indices

The annual fluctuations in SATVI provide context for the spatial and temporal magnitudes of a disturbance whether this be drought or fire. Additionally, the annual and seasonal fluctuations in SATVI at the control sites provide rich information on vegetation response to global and local climate cycles (Figure 8). Maxima in fractional vegetation cover are observed in April 2011 and April 2022, whereas the minimum mean fractional cover is found in November 2019 (Figure 8).

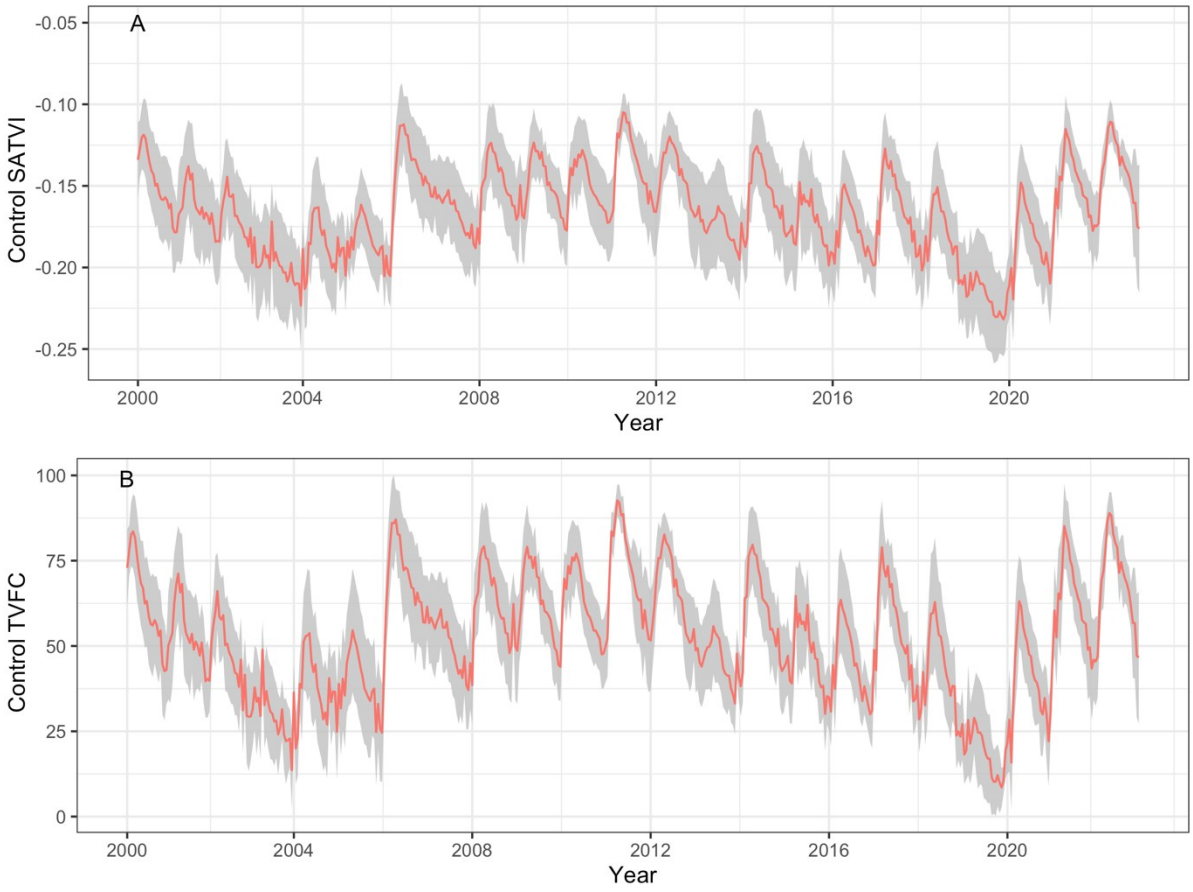

Figure 7. SATVI (A) and TVFC (B) for the control (unburned) pixels from 2000-2023. The one standard deviation is shown in grey and mean in red.

SATVI mean Total Vegetation Fractional Cover (TVFC) for the burned pixels show strong annual and seasonal fluctuations on the linear dunes in the research area (Figure 9b). Fire acts as a disruption to these fluctuations, reducing the mean TVFC by 54% (Figure 9b). However vegetative cover only reached its minimum fractional cover at five sites and the mean fractional cover minimum only drops to 19% after burning.

When compared to the control pixels, burned site recovery time varies (Figure 9c), the quickest time to achieve no difference between the burned and control site was 400 (±16) days which was recorded at three fires which burned in 2007 and 2011.

The longest time to recovery was 2528 (±16) days (around seven years) after a fire in 2013. The median time to return to a positive difference with the matched control site was 608 (±16) days. Although the TVFC values provide similar trends to the raw SATVI values (Figures 8 and 9), their weak correlation with ground measurements warrants focusing exclusively on the raw SATVI values.

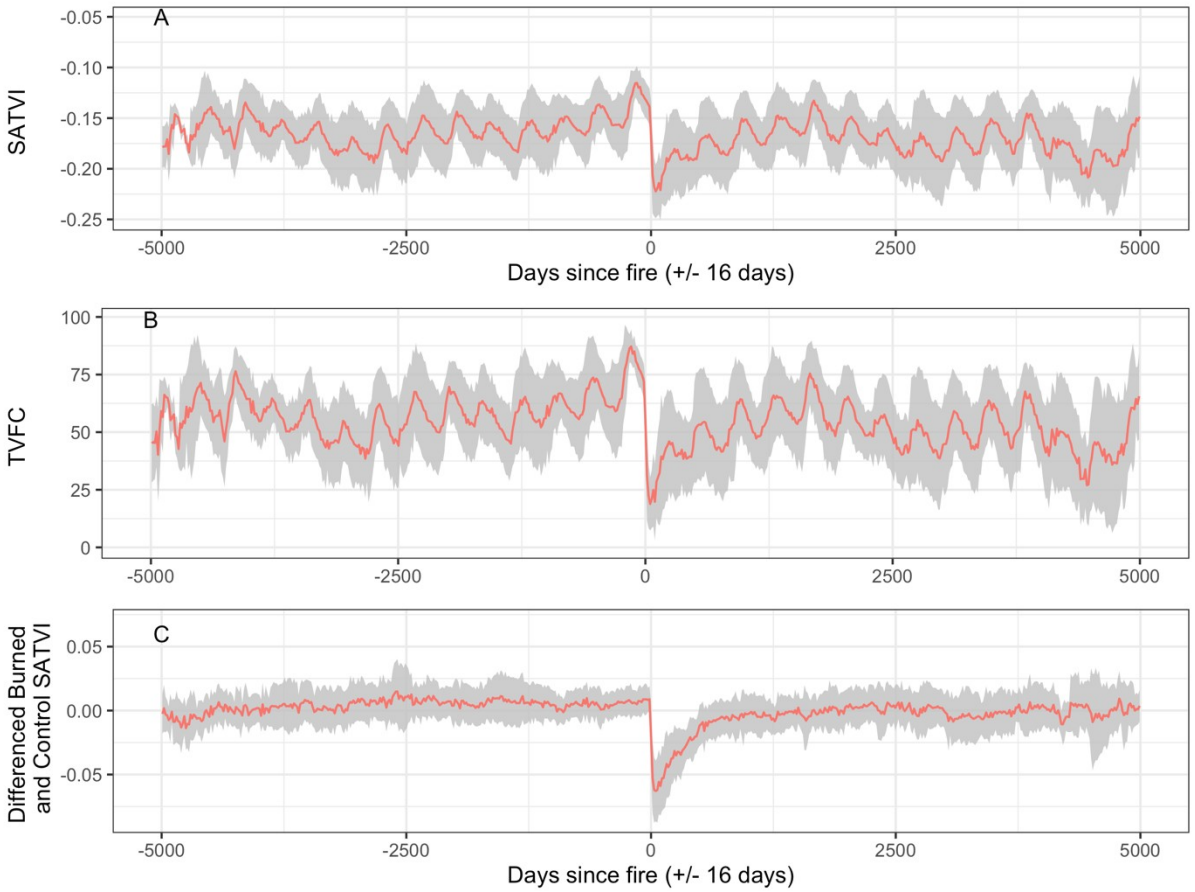

Figure 8. SATVI derived measurements of vegetation for 5000 days before and after fire. (A) displays raw SATVI values in the burned pixel before and after the 17 tracked fires. +/- one standard deviation is shown in grey and mean in red. (B) displays the same as (A) but for TVFC. (C) displays the difference in SATVI index between each paired burned and control pixel before and after fire.

5 Discussion

This study used MODIS burned area product to create an inventory of fire occurrence on an often-overlooked landscape, the Kalahari's southwest vegetated linear dunes. Scaling decisions in previous studies have resulted in this region being

omitted from global and continental-scale studies of burn-prone ecosystems (Archibald et al., 2009; Ramo et al., 2021; Roy et al., 2008). For example, Andela and Van Der Werf, (2014), excluded areas receiving less than 400 mm mean annual precipitation from their analysis of burn potential in African savannas. We show here that fires can be an important part of ecosystem dynamics, even in dryland dune regions. However, we also show that vegetation mostly recovers in under two years and in much of the study area fire was either triggered or suppressed by anthropogenic activity. As a result, fire as a disturbance effect, is limited both temporally and spatially and is not great enough to switch the system from a vegetated stable state to a de-vegetated stable state. These findings align with modelled scenarios for the Kalahari where, infrequent fire (10 years + reburn time) results in dune reactivation only 4% of the time (Mayaud et al., 2017).

This study evidences that fire is a large-scale disturbance factor in the southwest Kalahari despite previous under-representation. Nevertheless, some limitations should be acknowledged. Many satellite-derived BA products underestimate the amount of land burned, largely due to the lack of detection of small fires under 100 ha (Chuvieco et al., 2022; Khairoun et al., 2024; Ramo et al., 2021). In Sub-Saharan Africa, the MODIS BA only detected 5% of small fires, an uncertainty which is carried forward throughout this study (Ramo et al., 2021). In addition, the low spatial resolution of MODIS (~500m) means that the impact of dune morphology (i.e., the crest, flanks, and interdunes) on vegetation cover and fire spread could not be assessed in this work. Dune crests often remain sparsely vegetated after the vegetation reestablishment on the flanks and interdunes and aeolian activity may

534 persist here for some time (Wiggs et al., 1996). A more detailed discussion of the
535 impact that dune morphology can have on fire is provided in the supplementary
536 information (S3).
537
538 Further, whilst use of SATVI has proved more suitable for quantifying above-
539 ground total-biomass in arid and semi-arid environments (Marsett et al., 2006), the
540 index does not provide a complete ecological picture. SATVI does not record
541 changes in species composition or root biomass which can further impact aeolian
542 sediment transport and subsequent dune reactivation (Barchyn and Hugenholtz,
543 2013). Quantifying the influence that different canopies of vegetation (such as
544 shrubs, trees, and grasses) have on aeolian transport remains a persistent challenge
545 for aeolian research and is continuously being addressed through field and wind
546 tunnel studies (Kono and Okuro, 2021; Shumack et al., 2022). The quantification of
547 different vegetation types burned in this study would provide a more complete
548 assessment of the disturbance.

549 ## 5.1 The effect of fire on vegetation cover

550 By comparing SATVI values from burned and unburned control sites, we gained
551 information on post-fire recovery times across different years. Overall, the effect of
552 fire on vegetation fractional cover is short-lived: vegetation recovers quickly (Figure
553 9). All the sites returned to control fractional cover of vegetation, indicating that the
554 reduced-vegetation state was not a persistent change. The short period of reduced
555 vegetation cover limits the temporal window in which aeolian erosion can occur and
556 is much shorter than the previous disturbance window, of five years, suggested by
557 Wiggs et al. (1994). However, Wiggs et al. (1994) also investigated vegetation

structure as well as percent surface cover and accounted for this in the five-year recovery timeline.

Although a timeframe of two years is a useful indicator of vegetative state recovery it is not all encompassing, for example, high wind speeds may provide enough energy to remobilise sediment when the surface has not recovered to control levels. Indeed, Wiggs et al. (1995) found evidence of surface activity at up to 40% vegetation cover, although these were at low levels. TVFC only represents fractional cover and does not provide insights into the ground surface cover. Some burned pixels, for example on dune crests, may have consistently low surface vegetation cover which is further reduced when burned. The quick vegetation recovery time indicates that the saltating sand grains are not at a sufficient scale to abrade resprouting vegetation and create positive feedback mechanisms which limit vegetation recolonisation (Bhattachan et al., 2014). The lack of saltating grains may be due to vegetation cover not reducing enough to be sufficient for increased sediment transport (discussed below). Alternatively, other factors, such as the baking of the ground surface or biological soil crusts surviving being burned may leave the erodibility of the surface unchanged (Palmer et al., 2020). Additionally, the temporal window of erosion opportunity would have to match with climatic conditions conductive to aeolian erosion, dry and windy (Moritz et al., 2012), and thus the sites may also be erosivity limited in the immediate post-fire period.

5.2 Implications of anthropogenic controls on occurrence, size, and duration

583 In the southwest Kalahari vegetated dune field, land management systems have a
584 significant effect on fire occurrence and burn duration. This finding collaborates
585 previous results from southern Africa (e.g., Andela and Van Der Werf, 2014;
586 Archibald et al., 2009). One important finding is the comparison between the
587 primarily private farmland and the Kgalagadi Transfrontier Park, the latter of which
588 has a policy that naturally ignited fires are allowed to burn to their fullest extent
589 (Spies et al., 2016). This policy results in fires that often have long durations and
590 burn in multiple directions (Figure 3; Spies et al., 2016). In contrast to the Kgalagadi
591 Transfrontier Park, the agricultural lands in Namibia and South Africa have a high
592 volume of fire counts, but a much smaller burned area (Figure 5). One explanation
593 may be due to land users actively fighting the fires and having fire control methods
594 in place to reduce the affect that fire may have on agricultural potential and
595 livelihoods (Humphrey et al., 2021). A clear demonstration of these different fire
596 policies is the Namibian and South African border in the Kgalagadi Transfrontier
597 Park where a clear line has developed displaying how the fire is prevented for
598 traversing into neighbouring regions (Figures 3 and 7).
599
600 The anthropogenically modified fire regime in the southwest Kalahari dune field
601 severely limit the ability of fire to trigger dune activation. This is twofold. Firstly, the
602 small fires size reduces the area of sediment available to be moved. With only small
603 patches available to be eroded, the length is not sufficient to generate a large amount
604 of erodible material to produce significant surface activation (Miller et al., 2012).
605 Localised surface activation may occur, but this is limited by the continuing
606 vegetation and debris cover discussed above. Secondly, even though a quarter of

607 burns occur in the wet season, these fires do not have the right atmospheric or
608 ecological conditions to propagate (Jones et al., 2022), resulting in small fires that are
609 often restricted to a single day (Figure 3 and 5).
610
611 It is of interest that the highest number of fire days (Figure 3) and reburned pixels
612 (Figure 7) are recorded in the Nossob valley, where grass is much more limited than
613 on the dunes themselves (Leistner, 1959). The ephemeral river valley may act as a
614 natural fire break and prevent the burn spread. Fires burning the north and the
615 southeast side of the river often stop at the river valley. However, many of the pixels
616 that cover this region encapsulate both sides of the river and therefore return
617 frequent fires in that area. The river valley is also used as a road through the Park
618 and some burns originating in the valley may be triggered by human action. The
619 river valley also has a higher concentration of trees than the surrounding dunes
620 (Leistner, 1959). The trees provide optimal lightning strike features and can burn for
621 longer durations than grasses.
622
623 In addition, fires occur most commonly during (Figure 6) and 6-12 months after La
624 Niña conditions (Table 2). In arid regions, fuel quantity and continuity generally
625 govern fire regime (Archibald et al., 2009). As such, large fires only occur after
626 precipitation has been sufficient to promote biomass build up and continuity
627 (Andela and Van Der Werf, 2014). During La Niña phases, southern Africa has
628 wetter conditions (Mphale et al., 2014) which provides the moisture for biomass to
629 accumulate. In our data this is evidenced with the peaks in SATVI values during La
630 Niña conditions in 2006, 2011, and 2022 (Figure 8) which coincide (± one year) with

peaks in burn counts (Figure 4). The build-up of vegetation after precipitation is an explanation for why the 6 and 12 month lagged data shows a significant difference between ENSO phases and burn count and area (Table 2).

It is well known that humans influence fire regime (Andela and Van Der Werf, 2014; Kelley et al., 2019). In this region anthropogenic influences act to both suppress and ignite fires. The accidental ignition of fires are evident in the wet season fires, which would not occur naturally (Spies et al., 2016). However, the relatively small burned area of fires, even in the dry season is evidence of human suppression. If the Kgalagadi Transfrontier Park is taken as an example of a "natural" fire regime, fire will burn for longer and over a larger area than what we observe in the primarily private farmland. This finding highlights the importance of assessing the impact of fire and associated effects at both small and large spatial scales.

6 Conclusions

Our aim was to establish the scale of fire as a disturbance event on vegetated linear dunes by creating an inventory of burned area from 2000-2023 and quantifying post-fire vegetation regrowth. Overall, fires occur on all but three years and burn a significant amount of area on the vegetated dunes, but these burned areas are often limited to within the Kgalagadi Transfrontier Park and the wetter northern areas. We found that burn count and fire duration differs significantly between the Kgalagadi Transfrontier Park and primarily private farmland, which can be attributed to the differing fire management regimes, modulating the spatial scale of

the burn disturbance. In the primarily private land small, quick burning fires occur regularly, whilst in the National Park fires burn for longer, over larger areas, and more rarely. Vegetation regrowth also occurs rapidly after fire, limiting the temporal window for which post-disturbance sediment transport, and thus sediment activation, can occur. The temporal and spatial effect of the fire as a disturbance factor is limited by anthropogenic modulation (through land use practices) of the fire regime and rapid vegetation recovery post-burn. Due to the lack of representation of the southwest Kalahari dunes in fire studies, other vegetated dunes systems should also be reassessed and explored to understand fire dynamics and impacts upon these landscapes.

CRediT authorship contribution statement:

Rosemary Huck: Writing – original draft, Writing – review and editing, Conceptualization, Formal Analysis, Investigation, Methodology, Visualization. **David Thomas:** Writing – review and editing, Conceptualization, Methodology, Supervision. **Giles Wiggs:** Writing – review and editing, Conceptualization, Methodology, Supervision.

Declaration of competing interest:

The authors declare that they have no known competing financial interests or personal relationships that could have appeared to influence the work reported in this paper.

Data availability: The burned area data used in this study is publicly available from the NASA Fire Information for Research Management System (https://earthdata.nasa.gov/firms ; accessed on 19 May 2025). The MOD09GA data is available from NASA Land Processes Distributed Active Archive Center (https://lpdaac.usgs.gov/; accessed 19 May 2025). The ERA5-Land data can be downloaded from Copernicus (https://cds.climate.copernicus.eu/ ; accessed on 19 May 2025). ENSO data is available from the NOAA Climate Prediction Center (https://origin.cpc.ncep.noaa.gov/products/analysis_monitoring/ensostuff/ONI_v5.php ; accessed on19 May 2025)

Acknowledgements: We would like to thank NASA and the MODIS team alongside the EUMETSAT and NOAA teams for making the data publicly accessible.

Funding: This research was supported by the University of Oxford Clarendon Scholarship.

Reference list

Andela, N., Van Der Werf, G.R., 2014. Recent trends in African fires driven by cropland expansion and El Niño to la Niña transition. Nat. Clim. Chang. 4, 791–795. https://doi.org/10.1038/nclimate2313

Archibald, S., Roy, D.P., van Wilgen, B.W., Scholes, R.J., 2009. What limits fire? An examination of drivers of burnt area in Southern Africa. Glob. Chang. Biol. 15, 613–630. https://doi.org/10.1111/j.1365-2486.2008.01754.x

Barbosa, P.M., Stroppiana, D., Grégoire, J.M., Pereira, J.M.C., 1999. An assessment of vegetation fire in Africa (1981-1991): Burned areas, burned biomass, and atmospheric

emissions. Global Biogeochem. Cycles 13, 933–950.
https://doi.org/10.1029/1999GB900042
Barchyn, T.E., Hugenholtz, C.H., 2013. Reactivation of supply-limited dune fields from blowouts: A conceptual framework for state characterization. Geomorphology 201, 172–182. https://doi.org/10.1016/j.geomorph.2013.06.019
Bhattachan, A., D'odorico, P., Dintwe, K., Okin, G.S., Collins, S.L., 2014. Resilience and recovery potential of duneland vegetation in the southern Kalahari. Ecosphere 5, 1–14. https://doi.org/10.1890/ES13-00268.1
Bullard, J.E., Thomas, D.S.G., Livingstone, I., Wiggs, G.F.S., 1995. Analysis of linear sand dune morphological variability, southwestern Kalahari desert. Geomorphology 11, 189–203. https://doi.org/10.1016/0169-555X(94)00061-U
Burrows, N.D., Ward, B., Robinson, A., 2009. Fuel Dynamics and Fire Spread in Spinifex Grasslands of the Western Desert. Proc. R. Soc. Queensl.
Chuvieco, E., Mouillot, F., van der Werf, G.R., San Miguel, J., Tanasse, M., Koutsias, N., García, M., Yebra, M., Padilla, M., Gitas, I., Heil, A., Hawbaker, T.J., Giglio, L., 2019. Historical background and current developments for mapping burned area from satellite Earth observation. Remote Sens. Environ. 225, 45–64. https://doi.org/10.1016/j.rse.2019.02.013
Chuvieco, E., Roteta, E., Sali, M., Stroppiana, D., Boettcher, M., Kirches, G., Storm, T., Khairoun, A., Pettinari, M.L., Franquesa, M., Albergel, C., 2022. Building a small fire database for Sub-Saharan Africa from Sentinel-2 high-resolution images. Sci. Total Environ. 845. https://doi.org/10.1016/j.scitotenv.2022.157139
Giglio, L., Boschetti, L., Roy, D.P., Humber, M.L., Justice, C.O., 2018. The Collection 6 MODIS burned area mapping algorithm and product. Remote Sens. Environ. 217,

728 72–85. https://doi.org/10.1016/j.rse.2018.08.005
729 Goirán, S.B., Aranibar, J.N., Gomez, M.L., 2012. Heterogeneous spatial distribution
730 of traditional livestock settlements and their effects on vegetation cover in arid
731 groundwater coupled ecosystems in the Monte Desert (Argentina). J. Arid Environ.
732 87, 188–197. https://doi.org/10.1016/j.jaridenv.2012.07.011
733 Goudie, A.S., 2014. Desert dust and human health disorders. Environ. Int. 63, 101–
734 113. https://doi.org/10.1016/j.envint.2013.10.011
735 Goudie, A.S., 1991. Pans. Prog. Phys. Geogr. 15, 221–237.
736 Hao, Y., Hao, Z., Feng, S., Zhang, X., Hao, F., 2020. Response of vegetation to El
737 Niño-Southern Oscillation (ENSO) via compound dry and hot events in southern
738 Africa. Glob. Planet. Change 195, 103358.
739 https://doi.org/10.1016/j.gloplacha.2020.103358
740 Huck, R.A., Wiggs, G.F.S., Thomas, D.S.G., Wallum, N.S., 2025. Quantifying the
741 impact of fire events on dust emission potential from partially vegetated dunes in
742 the southwest Kalahari. Aeolian Res. 74, 101012.
743 https://doi.org/10.1016/j.aeolia.2025.101012
744 Hugenholtz, C.H., Wolfe, S.A., 2005. Biogeomorphic model of dunefield activation
745 and stabilization on the northern Great Plains. Geomorphology 70, 53–70.
746 https://doi.org/10.1016/j.geomorph.2005.03.011
747 Humphrey, G.J., Gillson, L., Ziervogel, G., 2021. How changing fire management
748 policies affect fire seasonality and livelihoods. Ambio 50, 475–491.
749 https://doi.org/10.1007/s13280-020-01351-7
750 Jones, M.W., Abatzoglou, J.T., Veraverbeke, S., Andela, N., Lasslop, G., Forkel, M.,
751 Smith, A.J.P., Burton, C., Betts, R.A., van der Werf, G.R., Sitch, S., Canadell, J.G.,

Santín, C., Kolden, C., Doerr, S.H., Le Quéré, C., 2022. Global and Regional Trends and Drivers of Fire Under Climate Change. Rev. Geophys. https://doi.org/10.1029/2020RG000726

Kaseke, K.F., Wang, L., Wanke, H., Turewicz, V., Koeniger, P., 2016. An analysis of precipitation isotope distributions across Namibia using historical data. PLoS One 11, 1–19. https://doi.org/10.1371/journal.pone.0154598

Kelley, D.I., Bistinas, I., Whitley, R., Burton, C., Marthews, T.R., Dong, N., 2019. How contemporary bioclimatic and human controls change global fire regimes. Nat. Clim. Chang. 9, 690–696. https://doi.org/10.1038/s41558-019-0540-7

Khairoun, A., Mouillot, F., Chen, W., Ciais, P., Chuvieco, E., 2024. Coarse-resolution burned area datasets severely underestimate fire-related forest loss. Sci. Total Environ. 920, 170599. https://doi.org/10.1016/j.scitotenv.2024.170599

Kolusu, S.R., Shamsudduha, M., Todd, M.C., Taylor, R.G., Seddon, D., Kashaigili, J.J., Ebrahim, G.Y., Cuthbert, M.O., Sorensen, J.P.R., Villholth, K.G., MacDonald, A.M., MacLeod, D.A., 2019. The El Niño event of 2015–2016: climate anomalies and their impact on groundwater resources in East and Southern Africa. Hydrol. Earth Syst. Sci. 23, 1751–1762. https://doi.org/10.5194/hess-23-1751-2019

Kono, A., Okuro, T., 2021. Spatial distribution of shrubs impacts relationships among saltation, roughness, and vegetation structure in an east asian rangeland. Land 10. https://doi.org/10.3390/land10111224

Leenders, J.K., van Boxel, J.H., Sterk, G., 2007. The Effect of Single Vegetation Elements on Wind Speed and Sediment Transport in the Sahelian Zone of Burkina Faso J. Earth Surf. Process. Landforms 32, 1454–1474. https://doi.org/10.1002/esp

Leistner, O.A., 1959. Notes on the vegetation of the Kalahari Gemsbok National Park

with special reference to its influence on the distribution of Antelopes. Koedoe. https://doi.org/10.4102/koedoe.v2i1.860

Levin, N., Levental, S., Morag, H., 2012. The effect of wildfires on vegetation cover and dune activity in Australia's desert dunes: A multisensor analysis. Int. J. Wildl. Fire 21, 459–475. https://doi.org/10.1071/WF10150

Livingstone, I., Thomas, D.S.G., 1993. Modes of linear dune activity and their palaeoenvironmental significance: An evaluation with reference to southern African examples. Geol. Soc. Spec. Publ. 72, 91–101. https://doi.org/10.1144/GSL.SP.1993.072.01.10

Manatsa, D., Reason, C., 2017. ENSO–Kalahari Desert linkages on southern Africa summer surface air temperature variability. Int. J. Climatol. 37, 1728–1745. https://doi.org/10.1002/joc.4806

Marsett, R.C., Qi, J., Heilman, P., Biedenbender, S.H., Watson, M.C., Amer, S., Weltz, M., Goodrich, D., Marsett, R., 2006. Remote sensing for grassland management in the arid Southwest. Rangel. Ecol. Manag. 59, 530–540. https://doi.org/10.2111/05-201R.1

Mayaud, J.R., Bailey, R.M., Wiggs, G.F.S., 2017. Modelled responses of the Kalahari Desert to 21st century climate and land use change. Sci. Rep. 7, 1–12. https://doi.org/10.1038/s41598-017-04341-0

Miller, M.E., Bowker, M.A., Reynolds, R.L., Goldstein, H.L., 2012. Post-fire land treatments and wind erosion - Lessons from the Milford Flat Fire, UT, USA. Aeolian Res. 7, 29–44. https://doi.org/10.1016/j.aeolia.2012.04.001

Moritz, M.A., Parisien, M.-A., Batllori, E., Krawchuk, M.A., Van Dorn, J., Ganz, D.J., Hayhoe, K., 2012. Climate change and disruptions to global fire activity. Ecosphere 3,

art49. https://doi.org/10.1890/es11-00345.1

Mphale, K.M., Dash, S.K., Adedoyin, A., Panda, S.K., 2014. Rainfall regime changes and trends in Botswana Kalahari Transect's late summer precipitation. Theor. Appl. Climatol. 116, 75–91. https://doi.org/10.1007/s00704-013-0907-z

Muñoz-Sabater, J., Dutra, E., Agustí-Panareda, A., Albergel, C., Arduini, G., Balsamo, G., Boussetta, S., Choulga, M., Harrigan, S., Hersbach, H., Martens, B., Miralles, D.G., Piles, M., Rodríguez-Fernández, N.J., Zsoter, E., Buontempo, C., Thépaut, J.N., 2021. ERA5-Land: A state-of-the-art global reanalysis dataset for land applications. Earth Syst. Sci. Data 13, 4349–4383. https://doi.org/10.5194/essd-13-4349-2021

Okin, G.S., Gillette, D.A., Herrick, J.E., 2006. Multi-scale controls on and consequences of aeolian processes in landscape change in arid and semi-arid environments. J. Arid Environ. 65, 253–275. https://doi.org/10.1016/j.jaridenv.2005.06.029

Okin, G.S., Parsons, A.J., Wainwright, J., Herrick, J.E., Bestelmeyer, B.T., Peters, D.C., Fredrickson, E.L., 2009. Do Changes in Connectivity Explain Desertification? Bioscience 59, 237–244. https://doi.org/10.1525/bio.2009.59.3.8

Palmer, B., Hernandez, R., Lipson, D., 2020. The fate of biological soil crusts after fire: A meta-analysis. Glob. Ecol. Conserv. 24, e01380. https://doi.org/10.1016/j.gecco.2020.e01380

Planet, T., 2017. Planet Application Program Interface: In Space for Life on Earth.

Poitras, T.B., Villarreal, M.L., Waller, E.K., Nauman, T.W., Miller, M.E., Duniway, M.C., 2018. Identifying optimal remotely-sensed variables for ecosystem monitoring in Colorado Plateau drylands. J. Arid Environ. 153, 76–87.

https://doi.org/10.1016/j.jaridenv.2017.12.008

Pricope, N.G., Binford, M.W., 2012. A spatio-temporal analysis of fire recurrence and extent for semi-arid savanna ecosystems in southern Africa using moderate-resolution satellite imagery. J. Environ. Manage. 100, 72–85. https://doi.org/10.1016/j.jenvman.2012.01.024

Ramo, R., Roteta, E., Bistinas, I., van Wees, D., Bastarrika, A., Chuvieco, E., van der Werf, G.R., 2021. African burned area and fire carbon emissions are strongly impacted by small fires undetected by coarse resolution satellite data. Proc. Natl. Acad. Sci. U. S. A. 118, 1–7. https://doi.org/10.1073/pnas.2011160118

Ravi, S., D'Odorico, P., Zobeck, T.M., Over, T.M., 2009. The effect of fire-induced soil hydrophobicity on wind erosion in a semiarid grassland: Experimental observations and theoretical framework. Geomorphology 105, 80–86. https://doi.org/10.1016/j.geomorph.2007.12.010

Roy, D.P., Boschetti, L., Justice, C.O., Ju, J., 2008. The collection 5 MODIS burned area product - Global evaluation by comparison with the MODIS active fire product. Remote Sens. Environ. 112, 3690–3707. https://doi.org/10.1016/j.rse.2008.05.013

Rykiel, E.J., 1985. Towards a definition of ecological disturbance. Aust. J. Ecol. 10, 361–365. https://doi.org/10.1111/j.1442-9993.1985.tb00897.x

Sankey, J.B., Germino, M.J., Glenn, N.F., 2012. Dust supply varies with sagebrush microsites and time since burning in experimental erosion events. J. Geophys. Res. Biogeosciences 117. https://doi.org/10.1029/2011JG001724

Shumack, S., Farebrother, W., Hesse, P., 2022. Quantifying vegetation and its effect on aeolian sediment transport: A UAS investigation on longitudinal dunes. Aeolian Res. 54, 100768. https://doi.org/10.1016/j.aeolia.2021.100768

Smit, M., Malan, P., Smit, N., Deacon, F., 2024. Response of herbaceous vegetation in the southern kalahari following a prolonged drought. J. Arid Environ. 222, 105157. https://doi.org/10.1016/j.jaridenv.2024.105157

Spies, A., Knight, M., Bradshaw, P., Ferreira, S., Bezuidenhout, H., Bissett, C., Wigley-Coetsee, C., Govender, D., Zimmerman, D., Hofmeyr, M., Smit, I., Govender, N., Smith, S., Conradie, L., van Eeden, B., Kruger, J., Viljoen, A., Ferreira, M., Titus, M., Makondo, K., Riley, A., Daemane, E., Peterson, R., Cole, N., Dreyer, B.-J., Waterston, K., Isaks, A., Mhlongo, E., Moolman, L., 2016. Management Plan Kalahari Gemsbok National Park 132.

Strong, C.L., Bullard, J.E., Dubois, C., McTainsh, G.H., Baddock, M.C., 2010. Impact of wildfire on interdune ecology and sediments: An example from the Simpson Desert, Australia. J. Arid Environ. 74, 1577–1581. https://doi.org/10.1016/j.jaridenv.2010.05.032

Sweeney, M.R., Lacey, T., Forman, S.L., 2023. The role of abrasion and resident fines in dust production from aeolian sands as measured by the Portable in situ Wind Erosion Laboratory (PI-SWERL). Aeolian Res. 63–65, 100889. https://doi.org/10.1016/j.aeolia.2023.100889

Swetnam, T.W., Betancourt, J.L., 1990. Fire-Southern Oscillation Relations in the Southwestern United States. Science (80-.). 249, 1017–1020.

Thomas, A.D., Dougill, A.J., 2007. Spatial and temporal distribution of cyanobacterial soil crusts in the Kalahari: Implications for soil surface properties. Geomorphology 85, 17–29. https://doi.org/10.1016/j.geomorph.2006.03.029

Van Der Werf, G.R., Randerson, J.T., Giglio, L., Collatz, G.J., Mu, M., Kasibhatla, P.S., Morton, D.C., Defries, R.S., Jin, Y., Van Leeuwen, T.T., 2010. Global fire emissions

872 and the contribution of deforestation, savanna, forest, agricultural, and peat fires
873 (1997-2009). Atmos. Chem. Phys. 10, 11707–11735. https://doi.org/10.5194/acp-10-
874 11707-2010
875 van Rooyen, N., van Rooyen, M.W., 1998. Vegetation of the south-western arid
876 kalahari: An overview. Trans. R. Soc. South Africa 53, 113–140.
877 https://doi.org/10.1080/00359199809520381
878 Villarreal, M.L., Norman, L.M., Buckley, S., Wallace, C.S.A., Coe, M.A., 2016. Multi-
879 index time series monitoring of drought and fire effects on desert grasslands. Remote
880 Sens. Environ. 183, 186–197. https://doi.org/10.1016/j.rse.2016.05.026
881 Wasson, R.J., Nanninga, P.M., 1986. Estimating wind transport of sand on vegetated
882 surfaces. Earth Surf. Process. Landforms 11, 505–514.
883 Wiggs, G.F.S., Livingstone, I., Thomas, D.S.G., Bullard, J.E., 1996. Airflow and
884 roughness characteristics over partially vegetated linear dunes in the southwest
885 Kalahari Desert. Earth Surf. Process. Landforms 21, 19–34.
886 https://doi.org/10.1002/(SICI)1096-9837(199601)21:1<19::AID-ESP508>3.0.CO;2-P
887 Wiggs, G.F.S., Livingstone, I., Thomas, D.S.G., Bullard, J.E., 1994. Effect of vegetation
888 removal on airflow patterns and dune dynamics in the southwest Kalahari desert. L.
889 Degrad. Dev. 5, 13–24. https://doi.org/10.1002/ldr.3400050103
890 Wiggs, G.F.S., Thomas, D.S.G., Bullard, J.E., 1995. Dune Mobility and vegetation
891 cover in the southwest Kalahari Desert. Earth Surf. Process. Landforms 20, 515–529.